

A Strategy for the Study of Cerebral Amino Acid Transport Using Iodine-123-Labeled Amino Acid Radiopharmaceutical: 3-Iodo-alpha-methyl-L-tyrosine

Keiichi Kawai, Yasuhisa Fujibayashi, Hideo Saji, Yoshiharu Yonekura, Junji Konishi, Akiko Kubodera, and Akira Yokoyama

Faculty of Pharmaceutical Sciences, Science University of Tokyo, Tokyo, Japan and School of Medicine and Faculty of Pharmaceutical Sciences, Kyoto University, Kyoto, Japan

We examined the brain accumulation of iodine-123-iodo-alpha-methyl-L-tyrosine (^{123}I -L-AMT) in mice and rats. L-L-AMT showed high brain accumulation in mice, and in rats; rat brain uptake index exceeded that of ^{14}C -L-tyrosine. The brain uptake index and the brain slice studies indicated the affinity of L-L-AMT for carrier-mediated and stereoselective active transport systems, respectively; both operating across the blood-brain barrier and cell membranes of the brain. The tissue homogenate analysis revealed that most of the accumulated radioactivity belonged to intact L-L-AMT, an indication of its stability. Thus, ^{123}I -L-AMT appears to be a useful radiopharmaceutical for the selective measurement of cerebral amino acid transport.

J Nucl Med 1991; 32:819-824

Various mental disorders have been associated with alterations in cerebral amino acid metabolism (1); in schizophrenic patients, for example, a defect of tyrosine transport has been suggested (2). Although some studies on the use of radiolabeled amino acids with cyclotron-produced ultra short-lived radionuclides have been attempted (3), they are limited to PET centers; a radioiodinated amino acid, providing similar data, would offer wider applicability.

The multifunctional role of amino acids, participating not only in protein synthesis but also as substrate for various metabolic pathway, are well known (4). Our previous work indicated that the election of radioiodinated amino acid derivatives with metabolic selectivity or high active membrane transport affinity was possible (5,6).

In the present work, a search for radioiodinated tyrosine derivatives for the cerebral tyrosine transport is attempted. In the screening process, in vitro accumulation studies in rat brain slices, measurement of brain uptake index (BUI), and in vivo mouse biodistribution are followed by the analysis of metabolites. In a preliminary study, the radioiodinated monoiodotyrosine in its L- and D-form (L-MIT and D-MIT) and its noniodinated counterpart (^{14}C -L-tyrosine) are tested.

The initial part of the work provided the basis for a radioiodinated tyrosine derivative to be used for the measurement of cerebral tyrosine transport. In particular, the data on conformational isomerism and the enzymatic deiodination of amino acids appeared as important factors to be considered. Thus, methylation of the L-tyrosine is estimated as the most plausible approach for providing the needed stability; and the alpha-methylated derivative, the 3-iodo-alpha-methyl-L-tyrosine (I-L-AMT, Fig. 1) is chosen. Compatibility of this I-L-AMT is comparatively tested with its parent, L-MIT, molecule and its use as the radioiodinated agent for the selective measurement of cerebral amino acid transport is discussed.

MATERIALS AND METHODS

Preparation of ^{125}I -L-AMT and ^{123}I -L-AMT

Iodine-125-NaI was obtained from Amersham Japan and ^{123}I -NaI was provided by Nihon Medi-Physics, Japan. All other chemicals used were of reagent grade. Iodine-125-L-AMT and ^{123}I -L-AMT were prepared by the conventional chloramine-T method as follows. Chloramine-T (Aldrich) at a concentration of 2.0×10^{-8} mol in 10 μl of 0.05 M phosphate buffer (pH 6.2) was added to a mixture of L-AMT (1.0×10^{-8} mol, Aldrich) and carrier-free ^{125}I -NaI (7.4-37 MBq) in 35 μl of 0.4 M phosphate buffer (pH 6.2). To prepare ^{123}I -L-AMT, L-AMT (1.0×10^{-6} mol in 25 μl of 1 N phosphoric acid) and chloramine-T (2.0×10^{-6} mol in 20 μl of 0.4 M phosphate buffer) were added to 500 μl of carrier-free ^{123}I -NaI (74-111 MBq) solution adjusted to pH 10. The resultant solution was allowed to stand for 2 min, and 20 μl

Received Oct. 31, 1989; revision accepted Oct. 19, 1990.

For reprints contact: Keiichi Kawai, PhD, Faculty of Pharmaceutical Sciences, Science University of Tokyo, 12, Ichigaya Funagawara-machi, Shinjuku, Tokyo, 162, Japan.

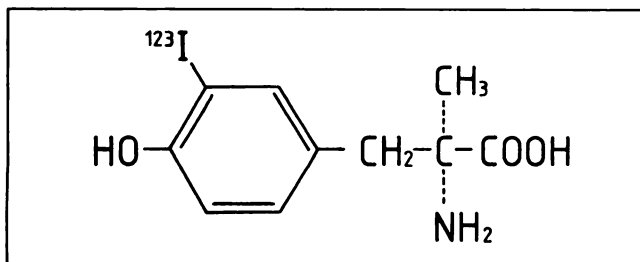


FIGURE 1. Structure of ^{123}I -3-iodo- α -methyl-L-tyrosine (^{123}I -L-AMT).

of 10% saturated sodium metabisulfite solution were then added. The radioiodinated L-AMT was purified by Sephadex LH-20 (Pharmacia) column chromatography (10 × 200 mm, eluant, ethylacetate:methanol:2 N ammonia = 40:10:4) (7). The labeling efficiency and radiochemical purity were studied by silica gel thin-layer chromatography (TLC, MERCK; Art. 5553) using two solvent systems, i.e., methanol: acetic acid = 100: 1 (Rf value: L-AMT, 0.50; I⁻, 0.75) and methanol: 10% ammonium acetate = 10: 1 (Rf value: L-AMT, 0.55; I⁻, 0.80).

As references, we used [U- ^{14}C]-L-tyrosine (NEN; NEC-289E) as a labeled natural amino acid, ^{125}I -3-iodo-L-tyrosine (^{125}I -L-MIT) and ^{125}I -3-iodo-D-tyrosine (^{125}I -D-MIT) prepared by the method mentioned above, and ^{123}I -N-isopropyl-p-iodoamphetamine ([^{123}I]IMP, Nihon Medi-Physics).

In Vivo Mouse Biodistribution Studies and Analysis of Metabolites

DdY male mice weighing 25 g received 0.1 ml of radioactive amino acids (^{125}I -L-AMT, ^{125}I -L-MIT, or ^{125}I -D-MIT at 1.6×10^{-13} mol and 11.1 kBq; ^{14}C -L-tyrosine at 4.0×10^{-10} mol and 7.4 kBq) via the tail vein and were then killed at various time intervals. For the measurement of radioactivity, a well-type scintillation counter (Aloka; ARC-300) was used for the ^{125}I - and ^{123}I -labeled compounds. For ^{14}C -L-tyrosine, 100 mg of tissue was dissolved in 1 ml of NCS tissue solubilizer (Amersham) and incubated at 50°C for 3 hr, followed by the addition of 8 ml of toluene scintillator containing DPO and POPOP. The radioactivity was measured using a liquid scintillation counter (Aloka; ARC-900).

An aliquot of tissue was homogenized and the 5% trichloroacetic acid-precipitated fraction was trapped on a glass filter (Toyo; GC-50) to allow measurement of the radioactivity incorporated in the protein. Furthermore, the tissue supernatant was separated by TLC using the solvents mentioned above to examine the metabolites.

Measurement of Partition Coefficients

The partition coefficients of ^{123}I -L-AMT, ^{14}C -L-tyrosine, and [^{123}I]IMP were measured using 2.0 ml of n-octanol as the organic phase and 2.0 ml of 0.1 M phosphate buffer as the aqueous phase (pH 7.0 for brain tissue and pH 7.4 for plasma). N-octanol and the buffer were pre-mixed twice using a mechanical mixer for 1 min at room temperature. Then, 20 μl of radioactive sample were added and mixed twice using a mechanical mixer for 1 min at room temperature. The radioactivity of 200 μl of each phase was measured after centrifugation.

Measurement of BUI

BUI studies were conducted based on the method reported by Oldendorf (8,9). Male Wistar rats weighing 250–300 g were

injected with 200 μl of saline containing 3.7 kBq of the radioactive sample and ^3H -H₂O via the right common carotid artery. The rats were decapitated 15 sec after injection, and the radioactivity of the right half of the brain rostral to the midbrain was measured. The BUI was calculated by the following equation:

$$\text{BUI} = \frac{\text{tissue } ^{125}\text{I or } ^{14}\text{C}/\text{tissue } ^3\text{H}}{\text{inj. soln } ^{125}\text{I or } ^{14}\text{C}/\text{inj. soln } ^3\text{H}} \times 100.$$

In competition studies, the injected solution contained 1×10^{-3} M cold L-tyrosine or L-AMT, a concentration that is about 14 times that of the endogenous tyrosine in normal rat plasma (10).

In Vitro Accumulation Studies in Rat Brain Slices

In vitro accumulation studies using rat brain slices were performed as previously reported (11). Male Wistar rats weighing 250–300 g were killed by decapitation and the brains were quickly dissected. The brain tissue was washed with ice-cold Krebs-Ringer phosphate buffer (pH 7.4) and then sliced with a conventional Stadie-Riggs slicer (12). The slices (each weighing 100 ± 5 mg) were next placed into a vial containing 1.9 ml of Krebs-Ringer phosphate buffer as the incubation medium and preincubated for 10 min for temperature equilibration. Then, 0.1 ml of the buffer containing a radioactive amino acid was added and incubation was performed at 37°C for 30 min. At the end of the incubation period, the medium was removed, and the slices were washed twice in 2 ml of ice-cold buffer. The radioactivity of the slices was then measured by the above-mentioned method. The percentage of the dose accumulated per gram of slice was calculated as follows:

Accumulation % dose/g slice

$$= \frac{\text{slice } ^{125}\text{I or } ^{14}\text{C}}{\text{inj. soln } ^{125}\text{I or } ^{14}\text{C} \times \text{slice weight}} \times 100.$$

Inhibition studies of the membrane active transport system were performed using incubation at 4°C and ouabain inhibition. For the ouabain inhibition study, brain slices were preincubated at 37°C for 20 min in medium containing 1×10^{-5} M of ouabain before addition of the radioactive sample. In the competitive inhibition studies, cold L- or D-tyrosine solution at a final concentration of 1×10^{-4} M and the radioactive samples were simultaneously injected. The final radioactive amino acid concentration was 2.7×10^{-11} M (1.85 kBq/ml, no-carrier-added) for ^{125}I -L-AMT and 1.0×10^{-7} M (1.85 kBq/ml) for ^{14}C -L-tyrosine.

RESULTS

Preparation of ^{125}I -L-AMT and ^{123}I -L-AMT

No-carrier-added ^{125}I -L-AMT and ^{123}I -L-AMT with radiochemical purities greater than 95% and radiochemical yields of 50%–60% were obtained after purification.

In Vivo Mouse Biodistribution Studies and Analysis of Metabolites

The brain accumulation of ^{125}I -L-AMT in mice is shown in Figure 2 compared with ^{125}I -L-MIT, ^{125}I -D-MIT, and ^{14}C -L-tyrosine. Comparison of ^{125}I -L-MIT with ^{125}I -D-MIT showed that the L-isomer exhibited higher brain accumulation than the D-isomer, indicating that stereoselectivity for the L-isomer occurred in the brain. The

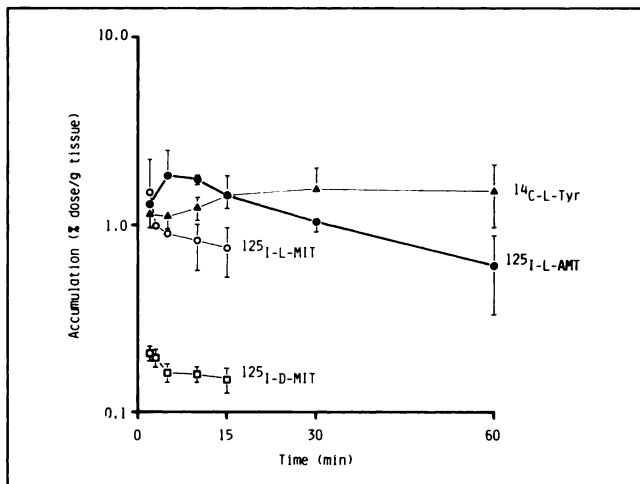


FIGURE 2. Brain accumulation of ^{125}I -L-AMT, ^{125}I -L-MIT, ^{125}I -D-MIT, and ^{14}C -L-tyrosine in mice. Each point represents the mean \pm s.d. of four to five animals. (●, ^{125}I -L-AMT; ○, ^{125}I -L-MIT; □, ^{125}I -D-MIT; ▲, ^{14}C -L-tyrosine).

alpha-methyl derivative, ^{125}I -L-AMT, showed higher accumulation than ^{125}I -L-MIT. Moreover, in the early stage up to 10 min after injection, ^{125}I -L-AMT showed superior uptake to its parent compound, ^{14}C -L-tyrosine, although after that ^{125}I -L-AMT levels rapidly decreased in the brain.

As shown in Figure 3, rapid clearance of ^{125}I -L-AMT from the blood was observed and the clearance curve was found to be similar to that of ^{125}I -D-MIT, which was stable against enzymatic deiodination (6). Redistribution in the blood, which was shown with ^{14}C -L-tyrosine, was not observed. As a result, 30 min after injection, ^{125}I -L-AMT showed lower blood levels than ^{14}C -L-tyrosine.

The chemical forms of the radioactive compounds in the mouse brain 10 min after injection are shown in Figure 4. Mice injected with ^{14}C -L-tyrosine exhibited less than

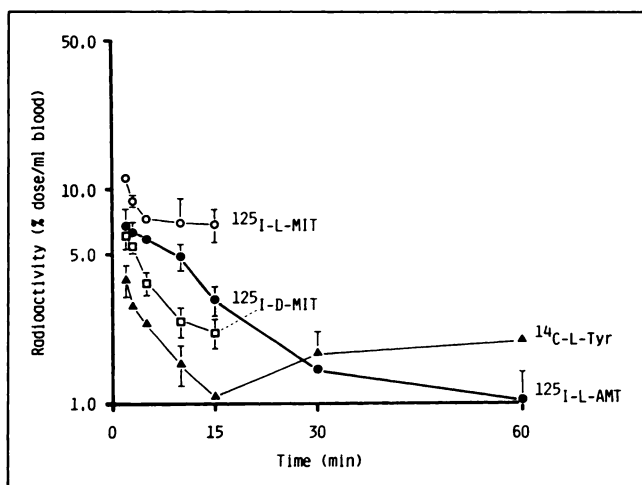


FIGURE 3. Clearance of ^{125}I -L-AMT, ^{125}I -L-MIT, ^{125}I -D-MIT, and ^{14}C -L-tyrosine from the blood in mice. Each point represents the mean \pm s.d. of four to five animals. Carbon-14-L-tyrosine was determined in plasma sample. (●, ^{125}I -L-AMT; ○, ^{125}I -L-MIT; □, ^{125}I -D-MIT; ▲, ^{14}C -L-tyrosine).

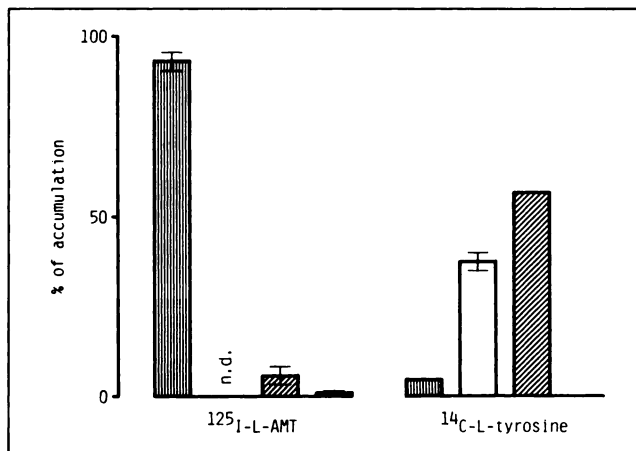


FIGURE 4. Fate of ^{125}I -L-AMT and ^{14}C -L-tyrosine in the mouse brain 10 min after injection. Each bar represents the mean \pm s.d. of three animals. Analysis for the amino acid and acid soluble metabolite fractions of ^{14}C -L-tyrosine are from only one animal. (Vertically striped bar, amino acid fraction; open bar, protein fraction; obliquely striped bar, acid soluble metabolite fraction; solid bar, free iodine fraction).

5% of the radioactivity in the brain as L-tyrosine, while 37.4% and 56.8% was found in the protein precipitate and the acid soluble metabolites, respectively. In the case of ^{125}I -L-AMT, more than 93% of the radioactivity in the brain was found as free amino acid, and not as protein or as free iodine. In Table 1, the percentages of radioactivity in the amino acid and free iodine fractions of ^{125}I -L-AMT in mouse tissues are shown compared with ^{125}I -L-MIT. In the case of ^{125}I -L-AMT, free iodine was about 1% of the radioactivity in the brain and less than 4% in the liver, kidney, and urine in contrast with ^{125}I -L-MIT.

Partition Coefficients

The partition coefficients of ^{123}I -L-AMT, ^{14}C -L-tyrosine, and [^{123}I]IMP are shown in Table 2. Iodination and methylation of the tyrosine molecule increased the lipophilicity to some extent, but the partition coefficient of ^{123}I -L-AMT was lower than that of [^{123}I]IMP, which is a well known lipophilic brain-seeking amine (13,14). Little difference of

TABLE 1
In Vivo Stability of Iodinated Amino Acids*

	^{125}I -L-AMT		^{125}I -L-MIT	
	AMT	Free I ⁻	MIT	Free I ⁻
Brain	93.02 (2.65)	1.08 (0.78)		
Liver	55.25 (7.05)	1.88 (1.34)	13.87 (2.90)	66.25 (5.39)
Kidney	94.93 (1.42)	2.21 (1.45)	14.07 (4.55)	75.07 (6.13)
Urine	93.09 (2.45)	3.81 (2.00)	4.79 (1.52)	94.21 (1.19)

* Ten minutes after intravenous injection, TLC analysis (MeOH:AcOH = 100:1).

TABLE 2
Partition Coefficients*

	pH 7.0	pH 7.4
$^{125}\text{I-L-AMT}$	-0.879 (0.003)	-0.911 (0.004)
$^{14}\text{C-L-tyrosine}$	-1.98 (0.02)	-2.00 (0.05)
$[\text{}^{123}\text{I}]\text{IMP}$	0.722 (0.026)	0.940 (0.008)

* $\log(\text{n-Octanol}/0.1 \text{ M phosphate buffer})$.

the partition coefficients between pH 7.0 and pH 7.4 was observed, in contrast with $[\text{}^{123}\text{I}]\text{IMP}$.

Brain Uptake Index

Iodine-125-L-AMT showed a high BUI of 62.1 ± 4.3 , in contrast with the 34.2 ± 4.7 observed for $^{14}\text{C-L-tyrosine}$ (Fig. 5). In addition, the brain uptake of $^{125}\text{I-L-AMT}$ was inhibited by the simultaneous injection of cold L-AMT or cold L-tyrosine, and a similar effect was detected with $^{14}\text{C-L-tyrosine}$.

In Vitro Accumulation Studies in Rat Brain Slices

The results of the accumulation and inhibition studies of $^{125}\text{I-L-AMT}$ and $^{14}\text{C-L-tyrosine}$ are shown in Figure 6. With incubation at 37°C for 30 min, $^{125}\text{I-L-AMT}$ ($158.4 \pm 9.4\%/g$) showed a similar accumulation to $^{14}\text{C-L-tyrosine}$ ($151.0 \pm 16.6\%/g$). With incubation at 4°C , the accumulation of both labeled amino acids was significantly decreased. Inhibition of accumulation was also detected in the presence of ouabain. In addition, stereoselective inhibition was detected only in the presence of cold L-tyrosine. These characteristics of $^{125}\text{I-L-AMT}$ were shared by $^{14}\text{C-L-tyrosine}$.

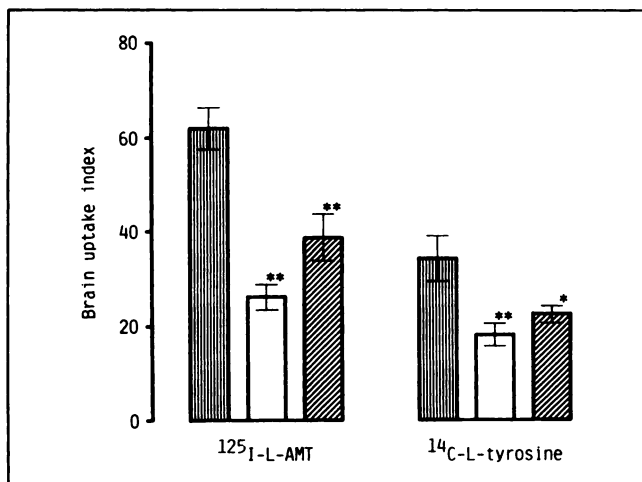


FIGURE 5. Brain uptake index of $^{125}\text{I-L-AMT}$ and $^{14}\text{C-L-tyrosine}$ determined in rats. Each bar represents the mean \pm s.d. of four to six animals. L-AMT and L-tyrosine were loaded at $1 \times 10^{-3} \text{ M}$. (Vertically striped bar, control BUI; open bar, L-tyrosine, and obliquely striped bar, L-AMT, at $1 \times 10^{-3} \text{ M}$ were added simultaneously). *, $p < 0.005$; **, $p < 0.001$.

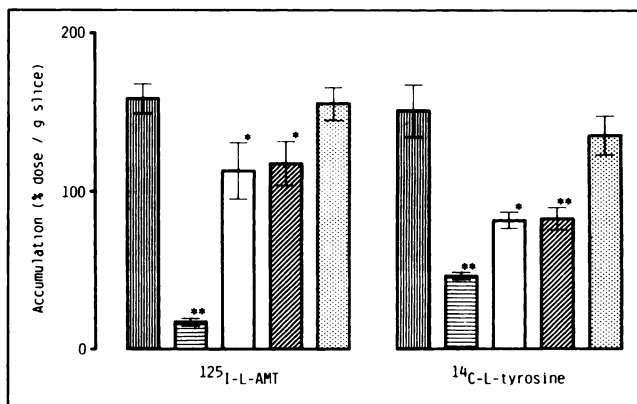


FIGURE 6. Inhibition of $^{125}\text{I-L-AMT}$ and $^{14}\text{C-L-tyrosine}$ accumulation in rat brain slices. Each bar represents the mean \pm s.d. of five experiments. (Vertically striped bar, samples incubated for 30 min at 37°C ; horizontally striped bar, samples incubated at 4°C ; open bar, samples loaded with $1 \times 10^{-5} \text{ M}$ ouabain and preincubated for 20 min; obliquely striped bar, L-tyrosine, and dotted bar, D-tyrosine, at $1 \times 10^{-4} \text{ M}$ were added simultaneously). * = $p < 0.005$, ** = $p < 0.001$.

DISCUSSION

Recent advances on PET brain studies have stimulated the search for radiopharmaceuticals for SPECT studies. Tyrosine or its derivatives have been radioiodinated or radiolabeled with positron-emitting radionuclides, but they have been used mostly for studies of protein synthesis or elucidation of biochemical pathways in normal or pathologic state (15-17).

Studies of cerebral amino acid transport are rare and only basic research has been reported, particularly with tyrosine (8,18). At first, basic experimentation was carried out with the radioiodinated tyrosine, MIT. The availability of radioiodinated MIT in its L- and D-form provided the preliminary basis for this work. In vivo biodistribution studies in mice showed high brain accumulation of the L-MIT, but not that of the D-MIT, a good indication of the well known stereospecificity of the blood-brain barrier, in the transport of neutral amino acids (8,18). However, tissue analysis revealed the metabolic instability of L-MIT, a metabolic intermediate of thyroid hormones, which is subjected to rapid enzymatic deiodination (19, 20). Use of a radioiodinated tyrosine derivative for amino acid transport studies requires an enzymatically stable derivative of L-MIT.

Methylation of L-MIT was considered since alpha-methylation has been reported to bring metabolic stability to the tyrosine molecule (21,22). Radioiodination of alpha-methyl substituted L-MIT was carried out and the metabolic stability of radiolabeled I-L-AMT needed for its brain transport measurement was screened.

In the early biodistribution stage, I-L-AMT showed higher brain accumulation than its non-methylated L-MIT and still higher, if compared with its parent $^{14}\text{C-L-tyrosine}$;

this difference was assessed by the BUI. These results indicated that not only methylation but the iodination of the tyrosine molecule induced no interference in the transport affinity of L-tyrosine into the brain.

The most interesting findings were obtained in the post-injection analysis of tissue metabolites. As expected, the presence of the methyl group in the alpha-position contributed to the stability of I-L-AMT against deiodination. TLC analysis revealed only 1%–2% of free iodine compared with 65%–75% in the case of L-MIT. On the other hand, a more systematic analysis of the brain homogenate revealed the presence of more than 80% of the radioactivity as unaltered I-L-AMT with a lack of participation in protein synthesis or other metabolic pathway, a distinctive behavior from its parent ^{14}C -L-tyrosine compound. Thus, the methylation in the alpha-position of the L-MIT might have induced the loss of the tyrosine molecule affinity for the metabolic pathway, but it kept the affinity for the transport system. This concept is supported by the very fast brain clearance of I-L-AMT observed 10–15 min postinjection, while the brain accumulation of the parent ^{14}C -L-tyrosine was still increasing.

The data suggest that non-metabolizable I-L-AMT provides one traceable characteristic of the parent L-tyrosine, which is valuable for the measurement of amino acid transport into the brain. To distinguish active transport from simple diffusion, characterization of I-L-AMT transport into the brain was performed. The *in vivo* as well as *in vitro* studies revealed that I-L-AMT transport across the blood-brain barrier is similar to its parent L-tyrosine (i.e., saturable or carrier-dependent, temperature-dependent, ouabain-inhibitable, and cross-inhibitable only by L-tyrosine). Due to the unavailability of the methylated D-form, no direct inhibition study could be performed, but the lack of inhibition with D-tyrosine might be considered as furnishing enough support for a stereospecific transport. In addition, the I-L-AMT n-octanol/phosphate buffer partition coefficient was too low for simple diffusion into the brain to occur by its lipophilicity (21), although the higher brain accumulation of I-L-AMT than its parent can be traced to the slightly higher value of its partition coefficient.

The structural requirements for amino acid transport into the brain are strict. The present methodical screening of tyrosine derivatives paved the way for the selection of I-L-AMT, as a radiopharmaceutical for brain tyrosine transport. Although I-AMT has already been reported as an imaging agent of the pancreas (24,25), melanoma (15, 26–28), or brain tumors (29), the stereoselective blood-brain barrier transport property, independent from the amino acid metabolism, might serve as a tool not only for the measurement of tyrosine transport in schizophrenia or other disease, but it also might be helpful in the building up of workable amino acid tracer kinetic models. Recently, human studies with ^{123}I - and ^{124}I -L-AMT have begun and good quality of brain images has been reported (30). The

present study will provide an important basis for the evaluation of I-L-AMT accumulation in human brain.

ACKNOWLEDGMENT

The authors wish to thank Nihon Medi-Physics Co. Ltd. for the generous supply of ^{123}I -NaI.

REFERENCES

1. Bustany P, Henry JF, Rotrou J, et al. Local cerebral metabolic rate of ^{14}C -L-methionine in early stages of dementia, schizophrenia, and Parkinson's disease. *J Cereb Blood Flow Metab* 1983;3(suppl):S492–S493.
2. Hagenfeldt L, Venizelos N, Bjerkenstedt L, Wiesel FA. Decreased tyrosine transport in fibroblasts from schizophrenic patients. *Life Sci* 1987;41:2749–2757.
3. Fowler JS, Wolf AP. Positron emitter-labeled compounds: priorities and problems. In: Phelps ME, Mazziotta JC, Schelbert HR, eds. *Positron emission tomography and autoradiography, principles and applications for the brain and heart*. New York: Raven Press; 1986:391–450.
4. McGilvery RW. Amino acids: disposal of nitrogen, amino acids: disposal of the carbon skeletons, amino acids: one-carbon pool and total balance, and amines. In: *Biochemistry, a functional approach*, international edition. Tokyo: Igaku-Shoin/Saunders; 1983:572–659.
5. Kawai K, Fujibayashi Y, Saji H, Konishi J, Yokoyama A. Metabolic studies of p-iodophenylalanine in pancreas: a gateway to the development of radioiodinated amino acid for functional diagnosis. *Jpn J Nucl Med* 1988;25:1263–1270.
6. Kawai K, Fujibayashi Y, Saji H, Konishi J, Kubodera A, Yokoyama A. Monoiodo-D-tyrosine, an artificial amino acid radiopharmaceutical for selective measurement of membrane amino acid transport in the pancreas. *Nucl Med Biol* 1990;17:369–376.
7. Williams AD, Freeman DE, Florsheim WH. Sephadex LH-20 column separation of thyroidal amino acids. *J Chromatog* 1969;45:371–380.
8. Oldendorf WH. Brain uptake of radiolabeled amino acids, amines, and hexoses after arterial injection. *Am J Physiol* 1971;221:1629–1639.
9. Oldendorf WH. Measurement of brain uptake of radiolabeled substances using a tritiated water internal standard. *Brain Res* 1970;24:372–376.
10. Scharff R, Wool IG. Concentration of amino acids in rat muscle and plasma. *Nature* 1964;202:603–604.
11. Yoshida H, Namba J, Kaniike K, Imaizumi R. Studies on active transport of L-DOPA (dihydroxyphenylalanine) into brain slices. *Jpn J Pharmacol* 1963;13:1–9.
12. Stadie WC, Riggs BC. Microtome for the preparation of tissue slices for metabolic studies of surviving tissues *in vitro*. *J Biol Chem* 1944;154:687–690.
13. Winchell SH, Baldwin RM, Lin TH. Development of I-123-labeled amines for brain studies: localization of I-123-iodophenylalkyl amines in rat brain. *J Nucl Med* 1980;21:940–946.
14. Kung HF, Tramposch KM, Blau M. A new brain perfusion imaging agent: [I-123]HIPDM: N,N,N'-trimethyl-N'-[2-hydroxy-3-methyl-5-iodobenzyl]-1,3-propanediamine. *J Nucl Med* 1983;24:66–72.
15. Kloss G, Leven M. Accumulation of radioiodinated tyrosine derivatives in adrenal medulla and in melanoma. *Eur J Nucl Med* 1979;4:179–186.
16. Bolster JM, Vaalburg W, Paans AMJ, et al. Carbon-11-labelled tyrosine to study tumor metabolism by positron emission tomography (PET). *Eur J Nucl Med* 1986;12:321–324.
17. Coenen HH, Kling P, Stöcklin G. Cerebral Metabolism of [2- ^{18}F] fluoro-tyrosine, a new PET tracer of protein synthesis. *J Nucl Med* 1989;30:1367–1372.
18. Oldendorf WH. Stereospecificity of blood-brain barrier permeability to amino acids. *Am J Physiol* 1973;224:967–969.
19. Roche J, Michel R, Michel O, Lissitzky S. Sur la deshalogenation enzymatique des iodotyrosines par le corps thyroïde et sur son rôle physiologique. *Biochem Biophys Acta* 1952;9:161–169.
20. Stanbury JB, Kassenaar AAH, Meijer JWA. The metabolism of iodotyrosine. I. The fate of mono- and di-iodotyrosine in normal subjects and in patients with various diseases. *J Clin Endocrinol Metab* 1956;16:735–746.
21. Cooper JR, Bloom FE, Roth RH. Catecholamine. I. General aspects. In: *The biochemical basis of neuropharmacology*, fifth edition. New York: Oxford University Press; 1986:203–258.
22. Mimnaugh MN, Gearien JE. Adrenergic drugs. In: Foye WO, ed. *Principles of medicinal chemistry*, third edition. Philadelphia: Lea & Febiger;

- 1989:343-358.
23. Levin VA. Relationship of octanol/water partition coefficient and molecular weight to rat brain capillary permeability. *J Med Chem* 1980;23:682-684.
 24. Tislar U, Kloster G, Ritzl F, Stöcklin G. Accumulation of radioiodinated L-alpha-methyltyrosine in pancreas of mice: concise communication. *J Nucl Med* 1979;20:973-976.
 25. Kloster G, Coenen HH, Szabo Z, Ritzl F, Stöcklin G. Radiohalogenated L-alpha-methyltyrosine as potential pancreas imaging agents for PECT and SPECT. In: Cox PH, ed. *Progress in radiopharmacology, volume 3*. Den Haag: Martinus Nijhoff; 1982:97-107.
 26. Bockslaff H, Kloster G, Stöcklin G, et al. Studies on L-3-[¹²³I]iodo-methyl tyrosine: a new potential melanoma-seeking compound. *Nuklearmedizin* 1980;(suppl 17):179-182.
 27. Bockslaff H, Kloster G, Dausch D, et al. First clinical results using L-3-¹²³I-alpha-methyl tyrosine for non-invasive detection of intraocular melanoma. *Nuklearmedizin* 1981;(suppl 18):840-844.
 28. Bockslaff H, Spitznas M, Hahn I, Kloster G. Noncontact detection of experimental amelanotic ocular melanoma with L-3-¹²³I-iodo-alpha-methyltyrosine. *Albrecht v Graefes Arch Klin Ophthal* 1981;217:255-266.
 29. Biersack HJ, Coenen HH, Stöcklin G, et al. Imaging of brain tumors with L-3-[¹²³I]iodo-alpha-methyltyrosine and SPECT. *J Nucl Med* 1989;30:110-112.
 30. Langen KJ, Coenen HH, Roosen N, et al. SPECT studies of brain tumors with L-3-[¹²³I]iodo-alpha-methyltyrosine: comparison with PET, ¹²⁴IMT, and first clinical results. *J Nucl Med* 1990;31:281-286.

(continued from page 802)

SELF-STUDY TEST

Gastrointestinal Nuclear Medicine

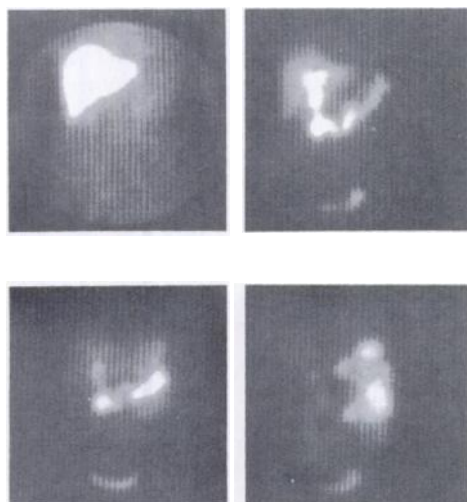


Figure 2B

- A. There is evidence for obstruction of the afferent (proximal) limb of the Billroth II reconstruction
- B. On the basis of the images alone, it can be concluded that entero-gastric reflux is responsible for the patient's symptoms.
- C. A calculated peak entero-gastric reflux index of 64% indicates that the patient's symptoms are likely to be relieved by surgical diversion of bile with a 45-cm Roux-en-Y limb.
- D. The patient's symptoms are likely related to post-operative gastroesophageal reflux.
- E. The absence of bilious vomiting makes it unlikely that the patient's symptoms are related to alkaline reflux gastritis.

ANSWERS

ITEM 1: Neonatal Jaundice

ANSWER: D

The initial angiographic phase with rapid sequential imaging is a useful component of hepatobiliary scintigraphy, in that unsuspected abnormalities, such as an arteriovenous malformation in the liver or renal inflammatory lesion, may occasionally be demonstrated. Avascular, photon-deficient areas within the liver may suggest cysts, dilated bile ducts as in Caroli's disease, or a choledochal cyst. There is no specific alteration in hepatic perfusion useful for distinguishing hepatocyte dysfunction from biliary atresia, however.

The kidneys are the alternate route of excretion of the ^{99m}Tc-IDA derivatives. Renal and bladder activity is prominent with either poor hepatic uptake and excretion (e.g., hepatitis), or good hepatic extraction but no excretion (biliary atresia). Normally, some renal and bladder activity is expected because, depending on the specific iminodiacetic acid derivative, 5%-15% of the injected dose will be excreted by the kidneys. The degree of renal excretion cannot be used to differentiate hepatocellular disease from an obstructive process.

In the newborn period, it is not usual to see good definition of the intrahepatic ducts, and visualization of the gallbladder is infrequent. When the gallbladder is seen, however, *intrahepatic* biliary atresia can be excluded. *Extrahepatic* obstruction is still possible, but dilatation of the bile ducts will often be evident by ultrasonography. Nonvisualization of the gallbladder is usual with impaired hepatocyte function and prolonged hepatic transit of the radiopharmaceutical. Thus, nonvisualization of the intrahepatic bile ducts and gallbladder may be seen with both hepatitis and biliary atresia, and these features cannot serve to distinguish these disorders.

In infants less than 3 months of age, assessing the degree of hepatic extraction may aid in differential diagnosis. Good extraction with a high liver-to-heart activity ratio at 5 minutes is suggestive of biliary atresia. Visually, there is rapid clearance from the blood pool with prominent hepatic uptake. Evaluation of the time-activity curves will confirm prompt uptake of tracer by the liver with either no washout over 60 minutes or a slight decrease after reaching peak activity. This is in keeping with the relatively good hepatocyte function at this stage. Beyond the age of 3 months, the effect of the prolonged obstruction on liver function becomes evident as hepatic extraction decreases. If the initial hepatic uptake is poor, then the patient is more likely to have neonatal hepatitis (or some other cause of hepatocellular dysfunction). Typically, the time-activity curve shows an early peak due to vascular activity. The shape of the curve parallels that of the cardiac blood pool, because there is minimal active uptake by the liver. With less severe hepatitis the extraction ratio is decreased. The curves show delayed uptake by the liver with a washout rate equal to or slightly greater than the rate of decrease in blood-pool activity. In the latter instance, excretion into the bowel may be anticipated in the delayed images. Thus, an evaluation of the early hepatic extraction and washout during the first 60 minutes may suggest the presence of biliary atresia or neonatal hepatitis, provided the patient is less than 3 months old.

References

1. Gerhold JP, Klingensmith WC II, Kuni CC, et al. Diagnosis of biliary atresia with radionuclide hepatobiliary imaging. *Radiology* 1983;146:499-504.
2. Majd M, Reba RC, Altman RP. Effect of phenobarbital on ^{99m}Tc-IDA scintigraphy in the evaluation of neonatal jaundice. *Semin Nucl Med* 1981;11:194-204.

(continued on p. 829)